

# FUNDAMENTAL PROPERTIES OF LIQUID ARGON, KRYPTON AND XENON AS RADIATION DETECTOR MEDIA

TADAYOSHI DOKE

Science and Engineering Research Laboratory, Waseda University, Kikuicho-17, Shinjuku-ku,  
Tokyo, Japan

(Received 23 June 1981)

**ABSTRACT** — The fundamental properties of liquid argon, krypton and xenon required from a point of view of radiation detector media, such as W-values, Fano factors, electron drift velocities, etc., have been measured during the past decade. These results are summarized and the author's considerations for its physical understanding are presented. Also, the possibilities of application of these liquids to nuclear radiation detectors are discussed.

## 1 — INTRODUCTION

Since Alvarez suggested the possibility of the use of liquefied rare gases, such as liquid argon or liquid xenon, as detector media of counters to be used in experiments of elementary particle physics [1], some trials for developing liquid argon or liquid xenon detectors were undertaken [2-9]. In the middle of the 1970's, liquid argon was successfully used as detector medium of calorimeters for high energy gamma-rays or electrons [10-15]. After a few years, a proposal of a «liquid argon time projection chamber» (LATPC), which is a new type three dimensional position sensitive detector with large sensitive volume and is used for neutrino detection, has been made by high energy physicists [16] and at present, the fundamental experiments for LATPC are in progress [17, 18].

Since the end of the 1960's, we began the studies on the fundamental properties of liquid rare gases [19-26] required for applications as radiation detector media, independently of Alva-

rez's suggestion, and recently have developed some new type liquid xenon detectors [27-30].

On the basis of the results obtained so far [19-30], in this article the fundamental properties of liquid rare gases as detector media are summarized and considerations are made regarding the physical understanding of their properties and the possibilities of application of these liquids to nuclear radiation detectors.

## 2 — IONIZATION

In the design of a liquid rare gas detector which is operated in the ionization mode it is necessary to know the mean number of ion pairs produced in the liquid by the ionizing radiation and its fluctuation around the mean value. The former can easily be estimated by knowing the  $W$ -value in the liquid, defined as the average energy required to produce an ion pair and the latter by knowing its Fano factor, which expresses the degree of fluctuation of the ionization.

Here, we will discuss the  $W$ -values and the Fano-factors of liquid argon, liquid krypton and liquid xenon recently measured or estimated by us and briefly describe the reasons why  $W$ -values in liquid rare gases are near the values in the gaseous state, rather than those in semiconductors, although Fano-factors are close to the values in semiconductors rather than those in the gaseous state.

### 2.1 — $W$ -values in liquid argon, krypton and xenon

For measurement of the  $W$ -value in liquid rare gases, the steady current method by irradiation with X-rays or alpha-rays has often been used by several investigators until recently [19, 20, 31-34]. However, this method is not suitable for precise measurement of  $W$ -values, because in X-ray irradiation, it is difficult to accurately determine the absorbed energy in the liquid medium and in alpha-particle irradiation, it is also difficult to completely collect the charge produced by alpha-particles. To overcome these difficulties of the measurement technique, we tried to use the electron pulse method and energetic conversion



electrons as ionizing radiation, for measurement of W-values in liquid rare gases [21, 22]. This method has the two following advantages: 1) the energy of individual pulses is known without any uncertainty, 2) the saturation of ionization pulses can easily be achieved because the specific ionization of energetic electrons is considerably low compared with that of alpha-particles. The W-values in liquid argon and liquid xenon obtained by this method are shown in Table 1, as well as those previously obtained by the steady current method [20]. From this table, it is clear that the accuracy of the determination of W-values by this method is remarkably improved, but the W-values obtained by both methods are in good agreement within the experimental errors.

TABLE 1 — The W values in the gas and liquid phases of argon, krypton and xenon. The number in parenthesis shows the ratio,  $W_{\text{gas}}/I$  or  $W_{\text{liq}}/E_g$ .

Liquid	I (eV)	$W_{\text{gas}}$ (eV) ( $W_{\text{gas}}/I$ )	$E_g$ (eV)	Experimental $W_{\text{liq}}$ (eV)		Calculated $W_{\text{liq}}$ (eV) ( $W_{\text{liq}}/E_g$ )
				Steady current method	Electron pulse method ( $W_{\text{liq}}/E_g$ )	
Ar	15.76	26.4 (1.68)	14.3	$23.7 \pm 0.7$	$23.6 \pm 0.3$ (1.65)	24.4 (1.70)
Kr	14.00	24.1 (1.72)	11.7	$20.5 \pm 1.5$		20.2 (1.72)
Xe	12.13	21.9 (1.81)	9.28	$16.4 \pm 1.4$	$15.6 \pm 0.3$ (1.68)	15.7 (1.69)

It is a well known fact that the ratios of W-values to ionization potentials in rare gases are nearly 1.7 and this was semi-quantitatively explained by Platzman on the basis of the result calculated for helium gas [35]. The existence of the electron band structure in solid rare gases, such as solid argon or solid xenon, has been already confirmed, but in the liquid state is confirmed only for liquid xenon. Let us assume that the same electron band structure as that in solid rare gases also exists in the liquid state. In this case, it is considered that the band gap energy  $E_g$  in the liquid state corresponds to the ionization poten-

tial I in the gaseous state. From such a view-point, in liquid rare gases, the ratio  $W/E_g$  of the W-value to the band gap energy will be used in place of the ratio  $W/I$  in the gaseous state. As seen from Table 1, however, the values of  $W/E_g$  in liquid rare gases are almost equal to the values of  $W/I$  in the gas state and differ from those in semiconductors such as silicon or germanium ( $\sim 3$ ). This fact can be explained from the phenomenological theory given by Shockley [36] and developed by Klein [37].

Namely, Shockley proposed the following relation for the balance of the energy dissipated in semiconductors in order to phenomenologically understand the ionization mechanism [35],

$$W = E_t^+ + E_t^- + E_i + r E_r, \quad (1)$$

where  $E_t^+$  and  $E_t^-$  are the mean energies of a subionization hole and electron respectively which are finally transferred to the lattice,  $E_i$  is the energy absorbed in production of an electron-hole pair, and  $rE_r$  is the energy transferred to the lattice while a free electron or a free hole, with energies higher than  $E_i$ , crosses the mean distance for electron-ion pair production. Assuming that the widths of the conduction band and the valence band are wider than the band gap and  $E_i$  is equal to  $E_g$ , Shockley derived the following formula for the W-value in a semiconductor (\*):

$$\begin{aligned} W &= 2 E_t + E_g + r E_r \\ &= 2 \times 0.6 E_g + E_g + r E_r \\ &= 2.2 E_g + r E_r \end{aligned} \quad (1')$$

After that, Klein obtained the following improved formula assuming that  $E_i = 3 E_g/2$ ,

$$W = (14/5) E_g + r E_r \quad (1'')$$

A good agreement between both values of  $dW/dE_g$  from the above formulas and the experimental results is obtained. By

---

(\*)  $0.6 E_g$  is obtained assuming that electrons or holes, with energies lower than  $E_i$ , distribute proportionally to their level density which is proportional to the square root of the kinetic energy.



fitting the formula (1'') to the experimental results,  $rE_r$  was estimated to be between 0.5 and 1.0 eV.

Now, let us apply such considerations to liquid rare gases, assuming that they have the same electron band structures as in solid state. In solid rare gases such as solid argon and xenon, there exists conduction band but no valence band. Therefore,  $E_f^+$  should be neglected. Since  $E_g$  is larger than ten times  $rE_r$ , we can also neglect the last terms in the formulas (1), (1') and (1''). Thus, we can obtain the following relation between the  $W$ -value and  $E_g$  in liquid rare gases,

$$W = 1.6 E_g \quad (\text{from Shockley's formula})$$

$$W = 1.9 E_g \quad (\text{from Klein's formula}).$$

These ratios (1.9 or 1.6) roughly agree with the experimental values of 1.65 for liquid argon [21] and 1.68 for liquid xenon [22]. More accurate estimation of  $W$ -values in liquid rare gases on the basis of the solid model will be made in the next section.

By admixing a small amount of a gas whose ionization potential is lower than the first excited state of the main gas, enhanced ionization is often observed in rare gases. Such a phenomenon is called Jesse effect. From the analogy with the Jesse effect in rare gases, it is expected that the same effect will occur in liquid rare gases. For example, the apparent ionization potential of a xenon atom doped in solid argon is 10.5 eV [38], which is lower than the energy of excitons in solid argon ( $\geq 12.0$  eV) [38]. This clearly shows that enhanced ionization is expected in xenon doped liquid argon. Actually, we observed such an enhanced ionization in the experiment of xenon doped liquid argon [24]. Figure 1 shows the variation of the ionization yield as a function of the doped xenon concentration. The enhanced ionization is also expected when some molecular gases are doped into liquid rare gases, but the mixing of molecular gases often leads to reduction of the pulse height of electron induced signals [23], because of the loss of electrons due to electron attachment to the molecular gases. Therefore, the observable enhancement of ionization may be limited to the case of mixing between rare gases.

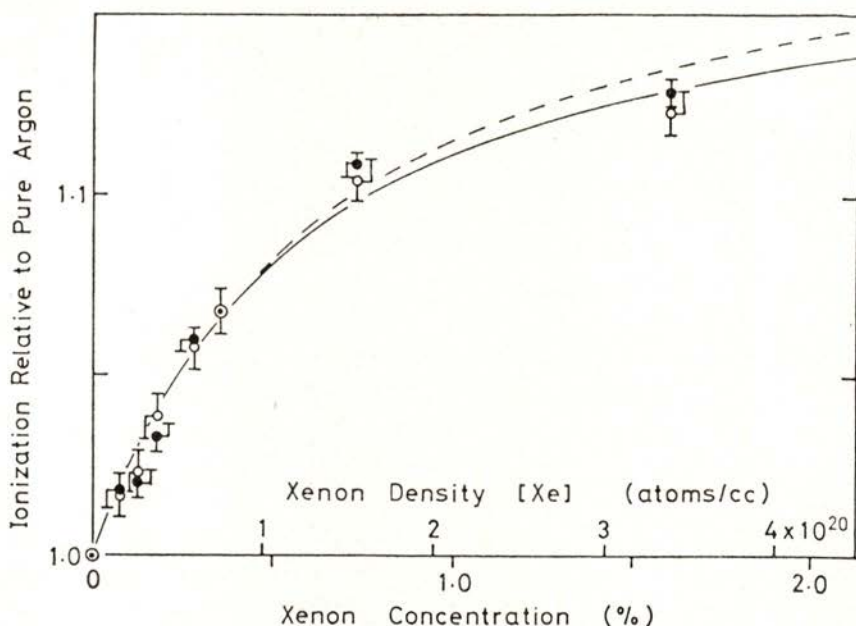


Fig. 1—Relative ionization yield as a function of the Xe concentration, for the ionization measured at 17 kV/cm(o) and for the saturation value estimated from the 1/I versus 1/E plot(•), where I is the ionization yield and E is the electric field.

## 2.2 — Estimate of W-values on the basis of the solid model

In this section, we describe more accurate estimations of W-values in liquid rare gases on the basis of the solid model. Namely, it is possible to accurately estimate the W-value in liquid rare gases, if its band structure and its oscillator strength are given. At present, we know the band structures in solid state obtained by theoretical calculation [39] and the oscillator strengths in solid state derived from the photo absorption spectra of these solid [40]. Assuming that these data are also applicable to liquid state, we try to estimate each term in the following energy balance equation previously applied to gases by Platzman [35]

$$W_1 / E_g = (E_i / E_g) + (E_{ex} / E_g) (N_{ex} / N_i) + (\epsilon / E_g), \quad (2)$$



where  $W_1$  is the W-value in liquid rare gas,  $N_{ex}$  is the number of excited atoms at an average expenditure  $E_{ex}$ ,  $N_i$  is the number of ions produced at an average energy expenditure  $E_i$  and  $\varepsilon$  is the average kinetic energy of subionization electrons. Here,  $E_i$  is estimated as a mean value of the gap energy in the electron momentum space. The ratios  $E_{ex}/E_g$  and  $N_{ex}/N_i$  are also estimated with the optical approximation using the oscillator strength spectra of solid rare gases. In these estimations, it is assumed that all the excitations which lie in the continuum above  $E_g$  dissociate to electron-hole pairs immediately. The estimation of the energy  $\varepsilon$  is made under the assumptions that the subionization electrons have energy less than  $E_i$  and distribute proportionally to the state density  $dn/dE$  for the energy levels. The results obtained in this way are shown in the last column of Table 1. The optical approximation used in this calculation is not valid for collisions due to low energy secondary electrons, which are a main part of collisions in the slowing down process of the primary particle. As seen from the table, nevertheless, the agreement between the estimated values and the experimental ones is very good.

From extrapolation of the enhanced ionization in xenon doped liquid argon to high concentration of xenon, the value of  $N_{ex}/N_i$  can be also estimated under the assumption that the excitons with energy higher than the ionization potential of the doped xenon atom contribute to the enhanced ionization. Then the estimated value of  $N_{ex}/N_i$  was  $0.19 \pm 0.02$  [24], which is in good agreement with that (0.21) used in the estimation of the W-value. This fact shows that the assumptions made in the estimation of W-values are reasonable. In the next section, therefore, we will try to estimate the Fano-factors in liquid rare gases by the use of the results obtained for the W-values.

### 2.3 — *Fano-factors in liquid rare gases*

The fundamental formula for the fluctuation of the number of ions produced by an ionizing particle when all its energy is absorbed in a stopping material was given by Fano [41]. For

convenience of calculation, the Fano's formula is transformed as follows [42, 43]:

$$\begin{aligned}
 F &= F_1 + F_2 + F_3 \\
 &= (N_{\text{ex}}/N_i) [1 + (N_{\text{ex}}/N_i)] (W_{\text{ex}}^2/W^2) + [(\varepsilon_i - W_i)^2/W^2] \\
 &\quad + (N_{\text{ex}}/N_i) [(\varepsilon_{\text{ex}} - W_{\text{ex}})^2/W^2] \quad (3)
 \end{aligned}$$

where  $W_{\text{ex}} = E_{\text{ex}}$ ,  $W_i = E_i + \varepsilon$ , and  $\varepsilon_i$  or  $\varepsilon_{\text{ex}}$  are the energy absorbed per ionization collision or per excitation collision in a large number of collisions in the slowing down process of an ionizing particle in matter, respectively. In this formula, the first term  $F_1$  is due to redistributions of the numbers of excited and ionized atoms, the second term  $F_2$  and the third term  $F_3$  are due to the energy loss fluctuations in ionization and excitation, respectively. In the calculation of Fano-factors, the values of  $N_{\text{ex}}/N_i$  and  $\varepsilon$  at the end of the ionization process should be used, because the fluctuation of the number of ion pairs produced by the ionizing particle is then determined and is not affected by the process of the excitation collisions after that. The values of  $N_{\text{ex}}/N_i$ ,  $E_i$ ,  $E_{\text{ex}}$  and  $\varepsilon$  at the end of the ionization process for liquid argon, krypton and xenon, obtained by the method described in the previous section, are given in Table 2. Table 3 shows the Fano-factors in liquid rare gases calculated from formula (3) by using these values and they are clearly small compared to those in the gaseous state. This is mainly attributed to the small values of  $N_{\text{ex}}/N_i$  in liquid state. From the view-point of detector application, in particular, it should be noted that the Fano-factors in liquid krypton and liquid xenon are comparable to those in semiconductors such as silicon and germanium.

TABLE 2—Quantities appearing in the energy balance equation for liquid argon, krypton and xenon.

Liquid	$E_i$ (eV)	$E_{\text{ex}}$ (eV)	$N_{\text{ex}}/N_i$	$\varepsilon$ (eV)
Ar	15.4	12.7	0.21	6.3
Kr	13.0	10.3	0.10	6.13
Xe	10.5	8.4	0.06	4.65



TABLE 3 —  $F_1$ ,  $F_2$ ,  $F_3$  and  $F$  (Fano-factor) in liquid argon, krypton and xenon for the solid model.

Liquid	$F_1$	$F_2$	$F_3$	$F$
Ar	0.076	0.027	0.004	0.107
Kr	0.032	0.024	0.001	0.057
Xe	0.019	0.021	0.0006	0.041

We can also estimate the Fano-factor in xenon doped liquid argon by using the formula for gas mixtures, derived by Alkhazov et al. [42]. The result is given by the following formula,

$$F_m = 0.107 - 0.067 \sigma,$$

where  $\sigma$  is the probability of deexcitation followed by an additional ionization. Considering the practical use as detector medium, therefore, we estimate the Fano-factor for xenon doped (1.6 %) liquid argon, whose ionization relative to that in pure liquid argon is 1.13 ( $\sigma \sim 0.68$ ),

$$F_m = 0.064.$$

#### 2.4 — *Energy resolution in liquid rare gas chambers*

Let us estimate the energy resolutions when these liquid rare gases are used as detector media in an ionization pulse chamber. In order to get the energy resolution of the chamber, first, the electronic noise level in the pulse amplification system must be given. We assume  $N_{n \text{ eq}} = 65e$  as the r.m.s. value of the noise equivalent charge in the electronic system, which can easily be achieved by using FETs (commercially available) kept at low temperature. If the  $W$ -value and the Fano factor for the detector media are known, the ultimate energy resolution  $\Delta E_T$ , which is

expressed by full width at half maximum (fwhm), is calculated from the following formula

$$\Delta E_T = (\Delta E_n^2 + \Delta E_j^2)^{1/2}$$

where  $\Delta E_n = 2,36 W$  (eV)  $N_{n\text{ eq}} \times 10^{-3}$  keV, and  $\Delta E_j = 2,36 \times \sqrt{E_\gamma}$  (MeV) FW (eV) keV and  $E_\gamma$  is the energy of ionizing radiation. The ultimate energy resolutions in liquid argon, liquid krypton and liquid xenon were calculated for  $E_\gamma = 1$  MeV, using the above formula. The results are shown in Table 4 [25]. From this table, it is clear that the ultimate energy resolutions for these liquid chambers are from 3 keV to 5 keV. In the conventional Ge(Li) detector with large volume, the actual energy resolution (fwhm) for gamma-rays of 1 MeV is about 1.5 keV. Therefore, the fwhm obtained in the liquid xenon ionization chamber is expected to be near that of the Ge(Li) detector. This encourages the development of a liquid xenon gamma-ray spectrometer.

TABLE 4 — Ultimate energy resolutions (fwhm) in liquid rare gas ionization chambers.

Liquid	$\Delta E_n$	$\Delta E_j$ (keV) for $E_\gamma = 1\text{MeV}$	$\Delta E_T$ (keV) for $E_\gamma = 1\text{MeV}$
Ar	3.57	3.77	5.19
Kr	2.99	2.49	3.89
Xe	2.36	1.88	3.02

In order to check the theoretical estimation as mentioned above, we tried to measure the energy resolution for 0.569 MeV gamma-rays emitted from  $^{207}\text{Bi}$  source using a small size liquid xenon gridded ionization chamber [22]. Figure 2 shows the relative energy resolution expressed by fwhm versus the electric field strength as well as the electronic noise level, corresponding to 17 keV, which is not so good. This curve is in fairly good agreement with that recently obtained by using a large volume liquid xenon chamber [29] and that of a Russian group using



a small size chamber [44]. From this figure, it is clear that the energy resolution (about 6% fwhm) is about twice the electronic noise level even for the electric field of 17 kV/cm, although the fwhm value still decreases with increase of the electric field.

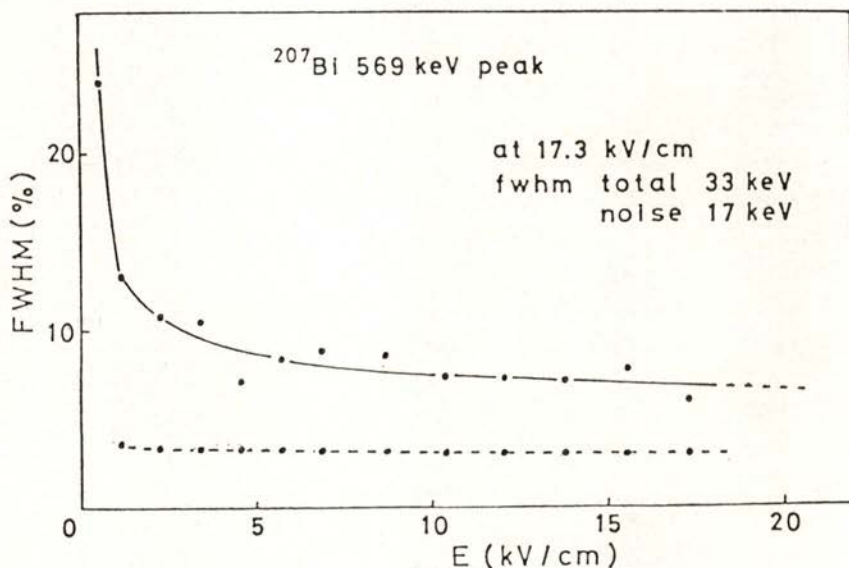


Fig. 2 — Variation of the energy resolution (fwhm) for gamma-rays of 569 keV with the electric field. Dashed line shows the level of electronic noise.

Such a large value of fwhm can not be attributed to attachment of electrons to electro-negative impurities in the liquid, because it had been experimentally shown that the pulse height of the ionization signals scarcely depends on the drift distance of electrons. Contributions to the energy resolution other than the electronic noise, such as the positive ion effect caused by the shielding inefficiency of the grid and the rise time effect of the ionization pulse, are considerably smaller than that of the electronic noise. Also, it may be difficult to explain such a large discrepancy between the theoretical estimation and the experimental results by the non-saturation effect of the collected charge for the applied electric field, because the difference between the collected charge at 17 kV/cm and its saturated value

obtained by Onsager's theory is estimated to be only 3% [22]. However, it is necessary to check whether the energy resolution is improved in much higher electric field or not, because at present the applicability of Onsager's theory to the ionization due to fast electrons in liquid rare gases is not sufficiently tested.

### 2.5 — *Electron multiplication in liquid and solid rare gases*

Several years ago, we tried to observe the occurrence of electron multiplication in liquid argon, and xenon doped or organic molecule doped liquid argon, by using a simple cylindrical counter with a center wire of about 5  $\mu\text{m}$  in diameter, but could not find it before electrical breaking occurs. To confirm the electron multiplication in solid argon or solid xenon as observed by Pisarev's group [45], furthermore, we also tried to test it using a parallel plate solid argon filament chamber [46]. In this test, a maximum multiplication factor of about ten was observed for a tungsten filament wire of 5  $\mu\text{m}$  in diameter. With increase of the anode voltage, however, the rise time of the output pulses became long and its decay time rapidly increased. At last, the pulses became unobservable because of pile-up. At present, these phenomena are interpreted assuming that the electron multiplication in solid argon occurs in a thin layer of gaseous argon near the wire surface and the slow component of the pulse is caused by space charge effect of electrons trapped in the imperfections of the interface between gas and solid. After these efforts, it was concluded that the electron multiplication to be useful in nuclear radiation detectors occurs only in liquid xenon as has already been confirmed by Derenzo et al [47].

The typical curves of charge gain versus applied voltage for a liquid xenon cylindrical counter with a center wire 5  $\mu\text{m}$  in diameter, obtained with internal conversion electrons from  $^{207}\text{Bi}$  and collimated  $^{137}\text{Cs}$  gamma rays, are shown in Fig 3 [48]. Here, the unit gain is equal to the saturated pulse height which is obtained in a small gridded ionization chamber filled with liquid xenon. The maximum gain obtained so far is about 200.



According to our experiences, the resolution of liquid xenon proportional counters becomes poor with the increase of the applied voltage. This degradation of resolution seems due to

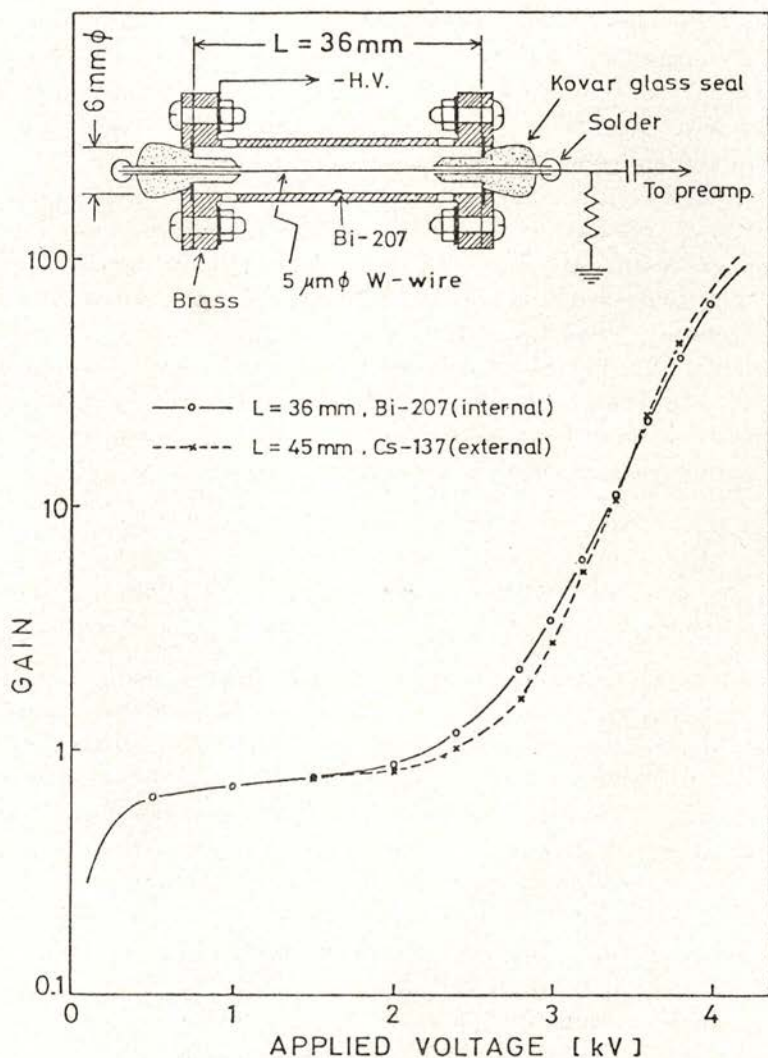


Fig. 3 — Charge gain versus applied voltage for a proportional counter having a center wire of  $5\text{ }\mu\text{m}$  in diameter, as shown in the inserted figure. The solid line represents the gain for an internal  $^{207}\text{Bi}$  source and the dashed line for external irradiation with collimated  $^{137}\text{Cs}$  gamma-rays.

local irregularities of the surface of the center wire. In practical applications of such a counter, this fact should be taken into consideration.

Derenzo et al. also tried to estimate the first Townsend coefficient in liquid xenon from their experimental data [3]. Namely they firstly derived the analytical formula for the variation of the charge gain with the applied voltage and fitted the curves obtained from the formula to the experimental data for three center wires of different diameter, by adjusting the values of  $W$ , recombination constant, attachment probability and first Townsend coefficient as unknown parameters. Then it was found that the first Townsend coefficient was 27 times larger than that in xenon gas with the same density as that of liquid xenon. However, this figure seems to be wrong, because the  $W$ -value and the recombination constant obtained as well as the first Townsend coefficient are inconsistent with those accurately measured by us [22, 23]. Therefore, we are trying to estimate the real value of the first Townsend coefficient by treating the  $W$ -value and the recombination constant as known parameters.

### 3 — RECOMBINATION AND ATTACHMENT

When an ionization chamber is used as an energy spectrometer for nuclear radiation, the charge produced by the ionizing radiation must be collected completely in the collector electrode in order to determine its intrinsic energy resolution. In the electron pulse chamber, the characteristics of electron charge collection are firstly determined by recombination between electrons and ions. In addition, the electrons attaching to electronegative gas during the drift to the collector can not effectively contribute to the induced voltage in the collector within the short measuring time, of the order of  $\mu$ sec. Therefore, the existence of electronegative gases in a liquid rare gas deteriorates the characteristics of the charge collection in an electron pulse chamber.

Here, we describe the present status in our understanding about the recombination and the attachment processes in liquid rare gases.



### 3.1 — *Recombination between electrons and ions*

If the electron-ion pairs produced by a minimum ionizing particle with low specific ionization are independent of each other, we can understand the recombination process between electrons and ions by Onsager's theory [49]. When an electron originated by ionization is slowed down to thermal energy, according to the theory, if the electron is within a certain distance from its parent ion where the Coulomb energy is equal to thermal energy, it can not escape from the influence of the parent ion and the electron-ion pair recombines. Conversely, if the thermalizing point of the electron is outside that critical distance, it is free from the influence of the parent ion even if the external electric field is zero. Actually, it seems that there exists a large number of free electrons, without recombination with the parent ion or other ions, during a considerably long time ( $>$ msec) in absence of electric field. However, it is difficult to completely understand the recombination process between electrons and ions in liquid rare gases only by Onsager's theory, because the mean interval of electron-ion pairs produced by ionizing radiation in liquids is comparable to the critical distance even for minimum ionizing particle and, under such a condition, the assumption of the existence of ion pairs which are independent of each other becomes unreal. Nevertheless, we consider that a rough explanation of the characteristics of charge collection in liquid rare gases is possible by Onsager's theory.

Figure 4 shows the characteristics of charge collection in liquid argon and liquid xenon observed by using internal conversion electrons of  $^{207}\text{Bi}$  [50]. In the figure, the solid curves are the theoretical ones obtained by fitting Onsager's theory to the experimental data and the agreement is good. According to Onsager's theory also, the initial slope of the charge collection curve in liquid xenon is smaller than in liquid argon.

However, the rise of the charge collection curve in liquid xenon is steeper than in liquid argon for electric fields lower than 1 kV/cm. This is different from the above prediction of Onsager's theory. Such a difference is caused by the effect of columnar recombination which occurs between electrons and ions other than the parent ion and the attachment of electrons to

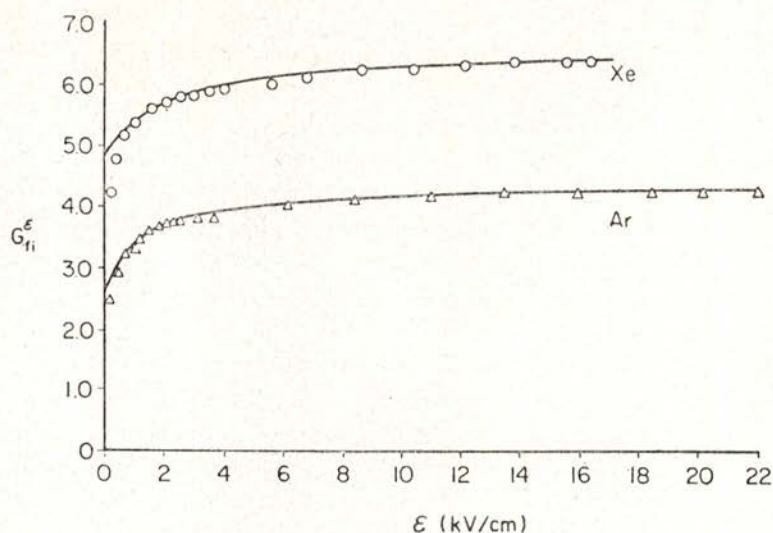


Fig. 4 — Saturation characteristics of collected charge versus electric field for liquid argon and xenon.  $G_{fi}^{\epsilon}$  is the free ion yield per 100 eV of absorbed energy at the field strength  $\epsilon$ .

electro-negative impurities in the rare gas liquid. By extrapolating the theoretical charge collection curve, obtained from the fitting to the experimental data for electric fields larger than 1 kV/cm, to the low electric field region, we can estimate the fraction of recombination free electrons to the total number of electrons produced by the radiation for zero electric field. The values obtained in this way are  $0.53 \pm 0.04$  for liquid argon and  $0.73 \pm 0.04$  for liquid xenon, respectively [50]. These values seem to be an overestimate, because of the ambiguity in the low electric field region. This problem will be again discussed in the section on direct scintillation.

### 3.2 — *Electron Attachment*

In an ionization chamber with a large sensitive volume, such as total absorption chambers or time projection chambers for neutrino detection, the electrons produced by ionizing radiation are required to drift a long distance without losses due to electron attachment to electro-negative impurities in the liquid



rare gases. From the point of view of the liquid argon time projection chamber, Chen et al. made an experiment to estimate how long electron drift lengths can be achieved in liquid argon supplied through a purifier, using a drift distance of a few centimeters, and showed that attenuation lengths longer than 35 cm are achievable at the electric field of 2 kV/cm [17]. Recently, they constructed a 50 liter liquid argon test chamber with a maximum drift distance of 30 cm and showed that an attenuation length of 55 cm is achievable at a drift field of 1.6 kV/cm [18]. Now, let us consider oxygen molecules as a typical electro-negative gas in liquid argon. Its cross section for electron attachment (or attenuation coefficient of drifting charge) in liquid argon at the electric field of  $10^2$  to  $10^4$  V/cm has already been measured by Zaklad [51], Hofmann et al [52] and Bakale et al [53].

Their results are shown in Figure 5 as well as the results in liquid xenon obtained by Bakale et al [53]. The values of

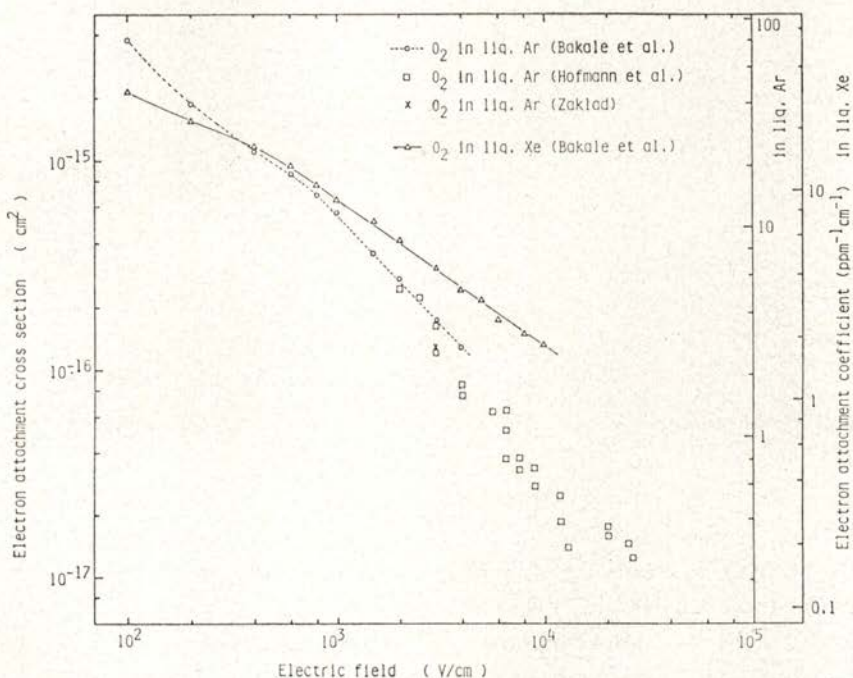


Fig. 5 — Variation of the electron attachment cross section with the electric field in liquid argon and xenon.

the electron attachment cross section in liquid argon are in good agreement. Using these values, the upper limit of the concentration of oxygen molecule in liquid argon used in Chen's experiment

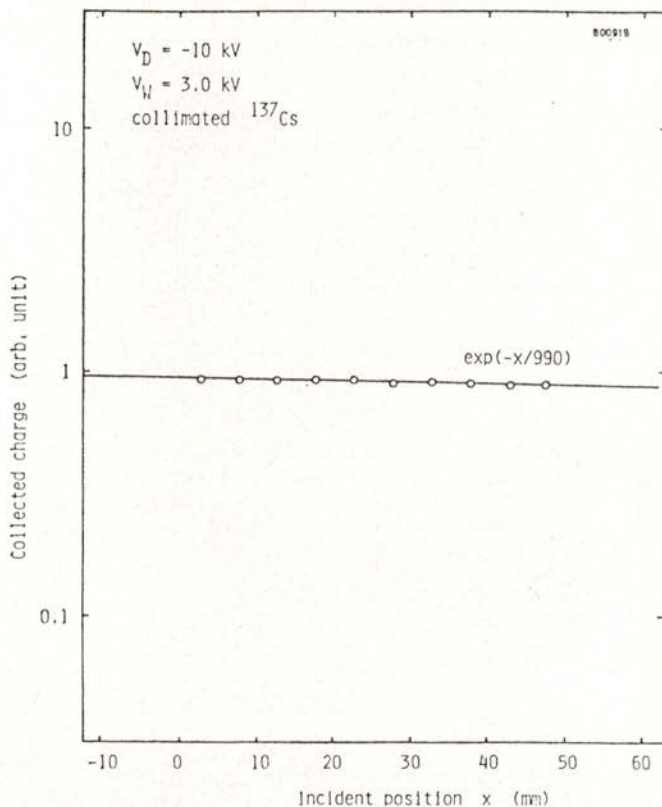


Fig. 6 — Attenuation of collected charge versus drifting distance in liquid xenon.

periment is estimated to be 2.6 ppb. Such a purity was obtained by passing a sequence of a Hydrox purifier and molecular sieves maintained at 196 K.

Complete collection of the charge produced by ionizing radiation in liquid xenon is more difficult than that in liquid argon, because a larger amount of electro-negative impurities are dissolved in liquid xenon due to a temperature higher than that



of liquid Ar [51]. In addition, the cross section for electron attachment by oxygen molecules is about one and a half times larger than that in liquid argon as seen in Fig. 5. Recently, we observed the reduction of the ionization pulse height for the drift distance of 5 cm in a liquid xenon drift chamber using collimated gamma-rays [30]. The result is shown in Figure 6. In this case, the attenuation length of electrons in liquid xenon was one meter. Assuming the cross section of electron attachment shown in Fig. 5, we can estimate the concentration of oxygen molecules in the liquid xenon used in our experiment to be 1.8 ppb, which is better than that obtained in liquid argon by Chen et al., in spite of the difficulty in purification of xenon. This shows that our test chamber and gas purification systems, in which a titanium-barium getter [48] is used, are superior to the systems of Chen et al.

#### 4 — ELECTRON DRIFT VELOCITY AND DIFFUSION

The drift velocity of electrons determines the time response of radiation detectors and the diffusion of electrons in the detector medium gives the limit of the accuracy of position determination. From the analogy with the mixing effect on the electron drift velocity in gaseous state, several years ago, we studied electron drift velocities in liquid argon mixed with small amounts of molecular gases and found a remarkable increase of the drift velocity for mixtures with methane or ethylene [23]. If the diffusion coefficient and the drift velocity of electrons in liquids are experimentally obtained as a function of the electric field strength, we can estimate the momentum transfer cross sections and the agitation (random) energies of electrons in the liquid state. This information gives us not only the spread of electrons drifting under an electric field in liquids, but also the understanding of the mixing effect as mentioned above. Therefore, we also tried to measure the diffusion coefficients of electrons in liquid argon [26, 57] and liquid xenon [57].

In this section, these results are shown and some relevant considerations are made.

4.1 — Electron drift velocities

As mentioned above, we measured the variations of electron drift velocities by admixing various kinds of molecular gases (200 to 5000 ppm) into liquid argon [23]. These results are shown in Figure 7 as well as the variation of the electron drift

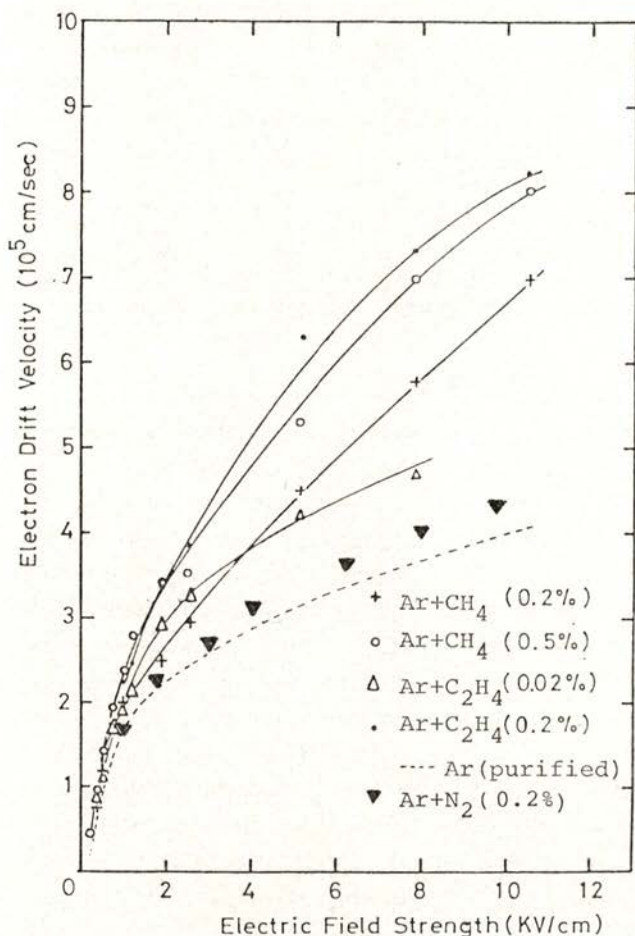


Fig. 7 — Variation of the drift velocity of electrons in liquid argon, liquid argon-nitrogen, -methane and -ethylene mixtures as a function of the electric field.



velocity for pure liquid argon as a function of electric field. As seen from the figure, in the liquid argon-nitrogen mixture, no significant change in the electron drift velocity was observed, while in liquid argon-methane and -ethylene mixtures, a considerable increase was observed. The degree of the increase in the electron drift velocity, however, is not so large as

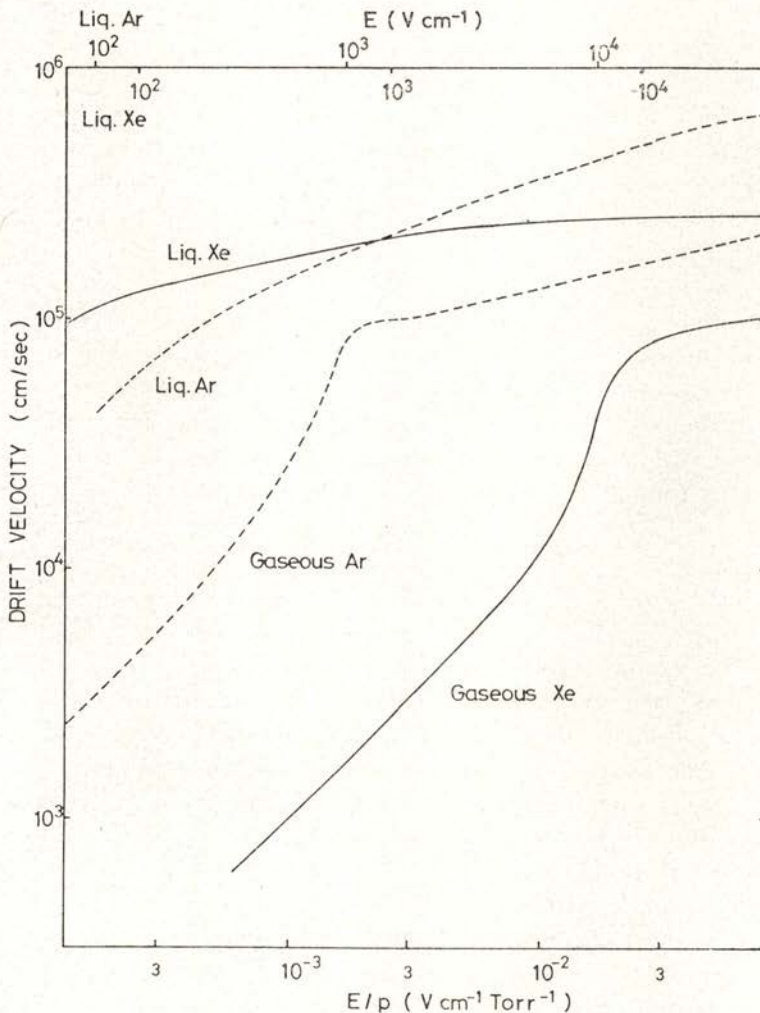


Fig. 8 — Variation of the drift velocity of electrons in liquid argon and xenon, and in gaseous argon and xenon with the same atomic density as in liquid state, with the reduced electric field.

expected directly from the analogy with the mixing effect in the gaseous state. This fact is due to the lack of the Ramsauer-Townsend effect in liquid argon as shown in the next section. Here, it should be noted that admixing of molecular gases into liquid rare gases results in a considerable reduction of pulse height. This is attributed to attachment of drifting electrons to electronegative gases included in the mixing molecular gas or in the rare gas itself. In applications of mixtures of liquid rare gases and molecular gases to detector media, great care must be taken regarding this problem.

Figure 8 shows the variations of the electron drift velocities in liquid xenon and liquid argon with the electric field for a wide range, as well as in gaseous argon and xenon with densities corresponding to the liquid state. These curves are drawn on the basis of the data recently obtained by several investigators [54, 55, 56]. From the figure, it is clear that the electron drift velocity in liquid is larger than that in gas over the whole region. In particular, the difference is remarkable in xenon. From the view-point of radiation detectors it should also be noted that liquid xenon is suitable as detector medium of drift chambers, because the electron drift velocity in liquid xenon is almost constant for electric fields higher than 3 kV/cm.

#### 4.2 — *Diffusion coefficient of electrons*

The group of electrons produced by the ionizing radiation in liquid rare gas gradually spreads during drifting along the lines of electric force by the diffusion process. The process is determined by the agitation velocity of electrons  $V_{ag} (\propto \langle \epsilon \rangle^{1/2})$ ,  $\langle \epsilon \rangle$  being the agitation energy) and the momentum transfer cross section of electrons  $\sigma$  in the liquid. If the spread of the electron group ( $\propto (Dt)^{1/2} = (Dd/\mu E)^{1/2} \propto (D/\mu)^{1/2}$ , where  $D$  is the diffusion coefficient,  $d$  the drift distance,  $\mu$  the mobility and  $E$  the electric field strength) in the liquid is measured as a function of the electric field, we can get the agitation energy of electrons from Einstein's relation  $eD/\mu = kT = 2\langle \epsilon \rangle/3$ . If we know the electron drift velocity or the electron mobility in the liquid, we can also get the diffusion coefficient of electrons by using that relation. Figure 9(a) and 9(b) show the variation



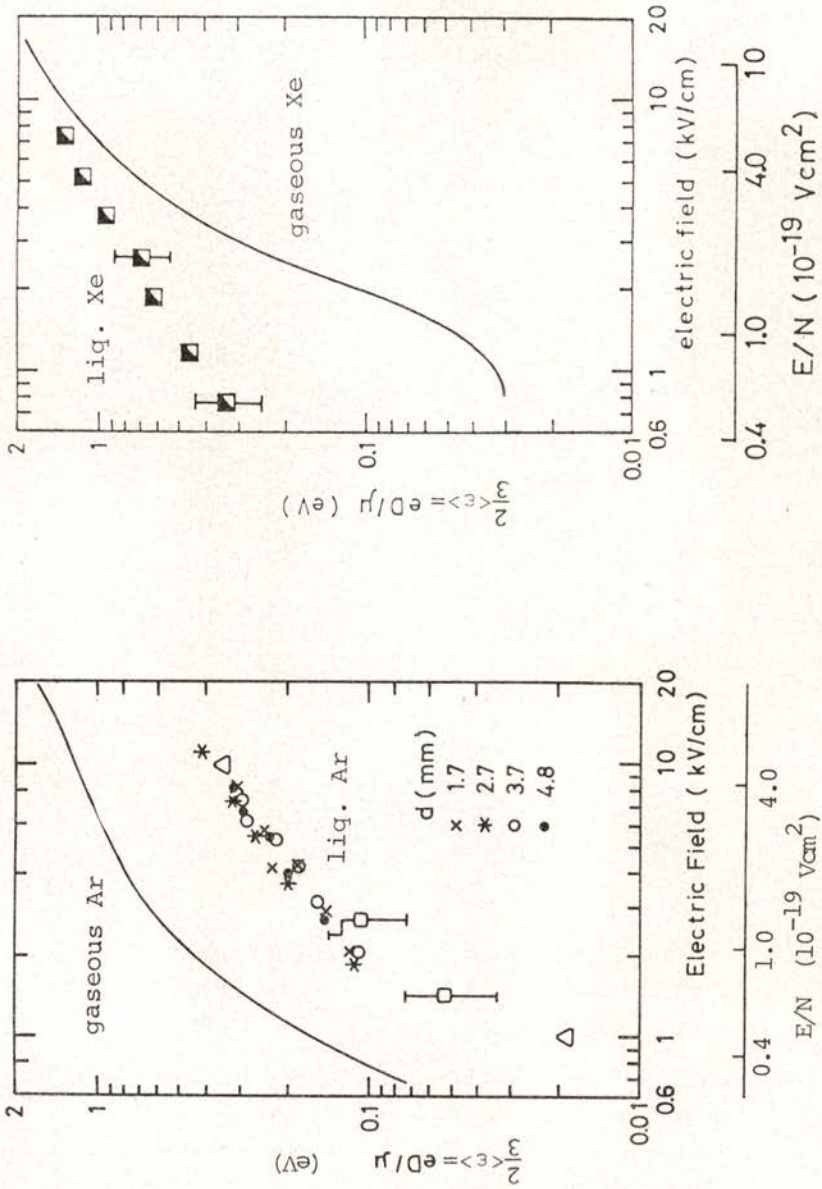


Fig. 9 — Field dependence of  $\frac{2}{3} \langle \epsilon \rangle = eD/\mu$  (eV) in liquid argon (a), and liquid xenon (b). Solid curves show the results for the gaseous states, respectively.  $N$ , in the lower horizontal scale, is the atomic density in the liquid state.

of  $\langle \epsilon \rangle$  in liquid argon and liquid xenon with the electric field strength obtained from measurements of the spread of electrons as mentioned above [26, 57]. For comparison with the agitation energy of electrons in gas, the curve for argon or xenon gas

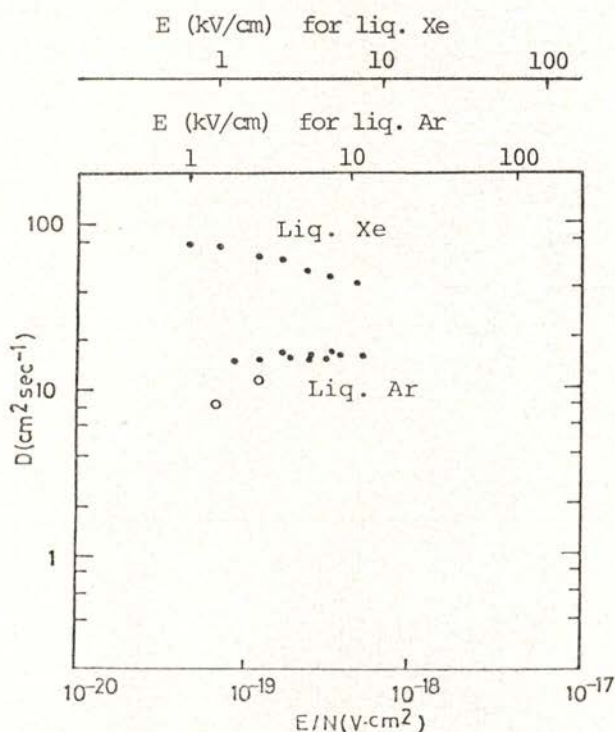


Fig. 10 — Field dependence of the diffusion coefficients of electrons.

with the same density as in the liquid state is also shown in each figure. As seen from the figures, the values of  $\langle \epsilon \rangle$  of electrons in liquid argon is several times lower than in gaseous argon, while those in liquid xenon is a few to ten times larger than in gaseous xenon.

Figure 10 shows the variation of diffusion coefficients of electrons in liquid argon and liquid xenon with the electric field



strength, which was obtained from the data of Fig. 9 (a) and (b). The diffusion coefficients in liquid argon are 10 to 20 cm<sup>2</sup>/sec for the electric field of 2 to 11 kV/cm and clearly smaller than those (17 to 37 cm<sup>2</sup>/sec) in gaseous argon with the same density as in the liquid state. This shows that liquid argon is superior to high pressurized gaseous argon as a detector medium for

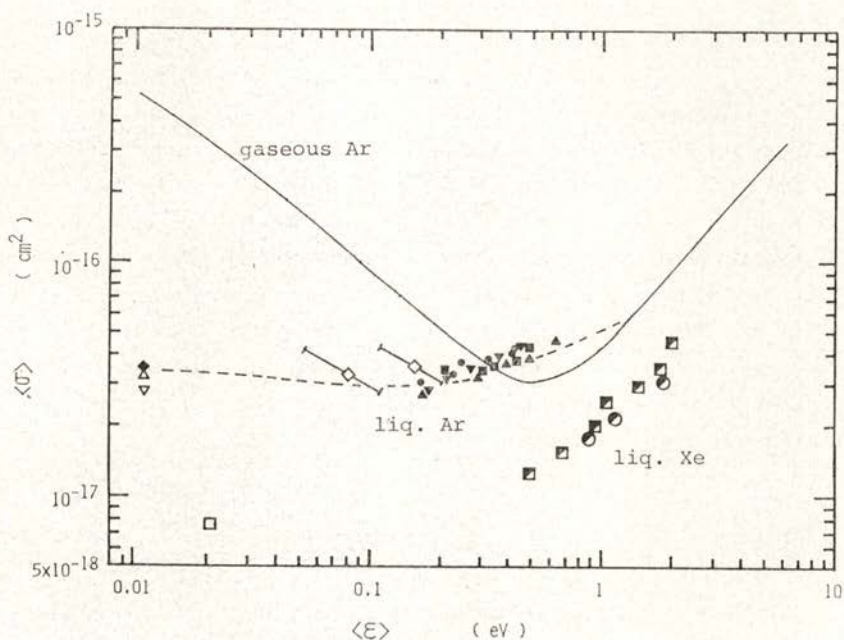


Fig. 11 — Variation of the momentum transfer cross section as a function of  $\langle E \rangle$  in liquid argon and xenon. The solid line shows the result for gaseous argon and the dashed line the result obtained by Lekner's theory.

position sensitive detectors. On the other hand, the diffusion coefficients in liquid xenon are several times larger than those in liquid argon. This means that the diffusion coefficient in liquid xenon is larger than that in gaseous xenon with the same density as in the liquid state, because the diffusion coefficient in gaseous xenon is smaller than in gaseous argon. Nevertheless, the diffusion coefficient in liquid xenon is still fifty times smaller

than that in xenon gas at one atmosphere and small enough to make negligible the fluctuation of the center of gravity of the electron cloud distribution, less than  $1 \mu\text{m}$  for the drift distance of 2 mm.

From the agitation energy  $\langle \epsilon \rangle$  of electrons and the electron drift velocity  $w$  or electron mobility  $\mu$ , we can estimate the momentum transfer cross section by using the simple formula  $\sigma_t = eE/Nw(2m\langle \epsilon \rangle)^{1/2}$ , derived from the relation  $w = eE\lambda/m\langle v \rangle$ , where  $N$  is the atomic density,  $e$  and  $m$  are the charge and mass of the electron, respectively,  $\lambda$  is the mean free path and  $\langle v \rangle$  is the average agitation velocity of the electrons. Figure 11 shows the variation of the momentum transfer cross sections of electrons in liquid argon and liquid xenon with the electric field strength, which was obtained from the above formula using the data shown in Fig. 9 (a) and (b). For comparison, the variation of the cross section with the electric field in gaseous argon with the same density as that of liquid argon is also shown by the solid line in the figure. This figure clearly shows the lack of the Ramsauer-Townsend minimum in liquid argon and liquid xenon as predicted by Lekner [58], compared with the curve for gaseous argon.

## 5 — SCINTILLATION

The scintillations in liquid rare gases due to ionizing radiations were studied by Northrop and Gursky [59], about twenty years ago. After that, however, such scintillations have been scarcely used in the field of nuclear experiments. Although it is sure that its application is not so easy as implied by Northrop and Gursky, the decay time of the scintillations from liquid rare gases such as liquid argon or xenon is very fast [64-68], and so they are useful as triggering pulses in the case of fast counting. Recently, furthermore, we found the so called proportional scintillation in liquid xenon [27, 28], which is the same phenomenon as that in rare gases. This finding will open the way to applications wider than that at the present. In this section, we describe some results on the direct scintillation and the proportional scintillation obtained in our experiments.



5.1 — *Direct scintillation*

Excited atoms  $R^*$  produced by ionizing radiation form excited molecules  $R_2^*$  through collision with other atoms on the ground state and ultraviolet photons are emitted in transitions from the lowest excited molecular state of  $R_2^*$  to the dissociative ground state. On the other hand, ionized atoms  $R^+$  produced by ionizing radiation also form excited molecules through the following processes: i)  $R^+ + R \rightarrow R_2^+$ , ii)  $R_2^+ + e \rightarrow R^{**} + R$ , iii)  $R^{**} \rightarrow R^*$  and iv)  $R^* + R \rightarrow R_2^*$  and then the excited molecules also give rise to ultraviolet photons. We call this type of scintillation «recombination scintillation». The mean wave lengths of these photons are 1300 Å for liquid argon, 1500 Å for liquid krypton and 1750 Å for liquid xenon, respectively.

The intensity ratio of scintillation from excited atoms to recombination scintillation will be given as  $N_{ex}/N_i$  if there is no radiationless transition process of the excited molecular state to the dissociative ground state, which does not seem to be theoretically probable for low temperatures as in liquid argon or liquid xenon. To justify such a theoretical consideration, we measured the variations of the scintillation intensities in liquid argon and liquid xenon as a function of electric field using internal conversion electrons from  $^{207}\text{Bi}$ . The results are shown in Figure 12 [60]. From this figure, it is clear that the scintillation intensity decreases with increase of the applied electric field, but even under electric fields higher than 10 kV/cm the scintillation intensities remain 32 % of that without the electric field for liquid argon and 26 % for liquid xenon. These values are larger than the theoretical values of 17 % for liquid argon and 5.7 % for liquid xenon, which are estimated from  $N_{ex}/N_i + N_{ex}$ . This discrepancy may be explained by taking into consideration the existence of recombination free electrons as mentioned in section 3. Namely, the recombination rate between recombination free electrons and ions is very slow and as the result, we can not observe the scintillation produced from such a recombination by the fast pulse techniques, which are widely used in the field of nuclear experiments. So, assuming that the recombination free electrons do not contribute to the scintillation, we can estimate the reduction factor of scintillation light to be 31 % for liquid argon and

18 % for liquid xenon, using the fractions of recombination free electrons obtained by the analysis on the basis of Onsager's theory [50]. These values roughly agree with the experimental ones.

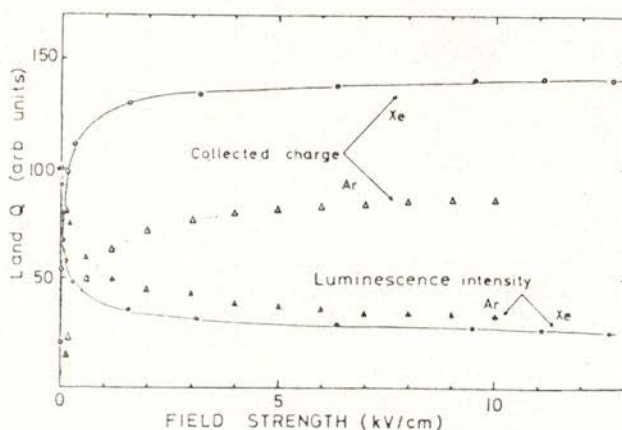


Fig. 12 — Variation of the relative luminescence intensity  $L$  and collected charge  $Q$  in liquid argon and liquid xenon with the applied electric field strength for 1 MeV electrons.

If the effect of recombination free electrons on the scintillation intensity in liquid rare gases is clear for fast electrons, it is considered that the scintillation yield per unit absorbed energy due to fast electrons may be smaller than that due to alpha-particles, which produce comparatively higher specific ionizations along the track where recombination efficiently occurs. To make sure of the matter, we tried to measure the  $dE/dx$  dependence of the scintillation yield in liquid argon using several kinds of ionizing particles [61, 62]. Figure 13 shows the results obtained. The data in the figure are normalized to the scintillation yield due to alpha-particles and show that the scintillation yield due to fast electrons is about 15 % lower than that due to alpha-particles. However, we could not observe the reduction of one-third in the scintillation yield due to alpha-particles. By using fission fragments from  $^{252}\text{Cf}$ , on the other hand, we found a great reduction of the scintillation yield in the high specific ionization region [61]. To compare with NaI (Tl) crystals, the



variation of the scintillation yield with the energy loss rate of the incident particle for those scintillators [63] is also shown by a solid curve in the same figure. As seen from

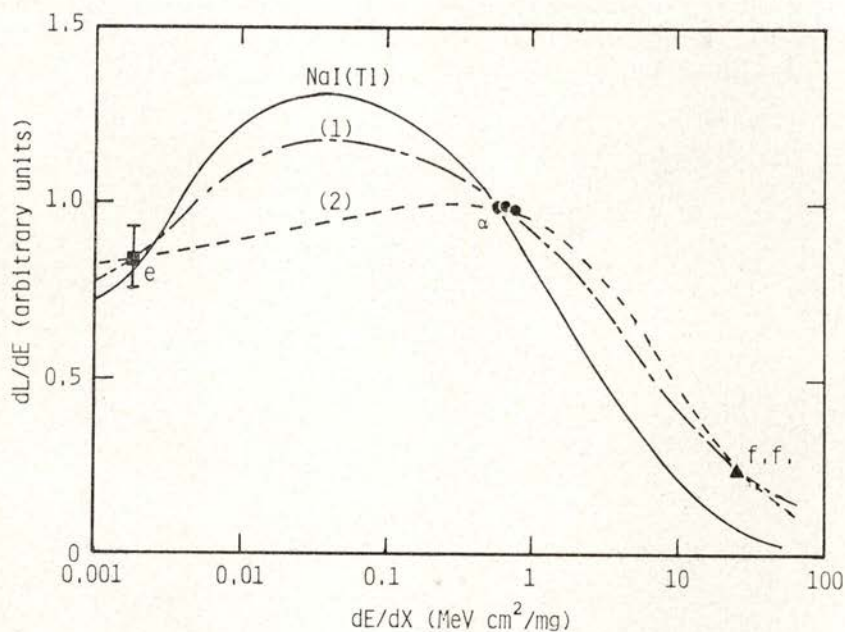


Fig. 13 — Scintillation yield per unit absorbed energy  $dL/dE$  as a function of the specific ionization  $dE/dx$  in liquid argon. Solid curve shows the  $dE/dx$ -dependence of scintillation yield in NaI(Tl) crystals. Scintillation yields in the figure are normalized to that due to alpha-particles. For dashed curves (1) and (2), see the text.

this figure, it seems that the experimental data naturally fit to the curve (1), like that for NaI (Tl) crystals, rather than to the curve (2), which is comparatively flat compared with curve (1). The peak seen in curve (1) may be explained by considering the effect of recombination free electrons in the low specific ionization region and the quenching effect in the high specific ionization region; and by the same considerations, the question why the scintillation yield due to fast electrons is only 15% lower than that due to alpha-particles may be

solved. To justify such a consideration, at present, we are planning to measure the scintillation yields due to protons of several tens MeV and other heavy ions.

Apart from the theoretical view point as mentioned above, let us compare the  $dE/dx$ -dependence of the scintillation yield in liquid argon with that in NaI (Tl) crystals. As a whole, the curve of scintillation yield versus  $dE/dx$  for liquid argon is comparatively flat compared with the curve for NaI (Tl) crystals.

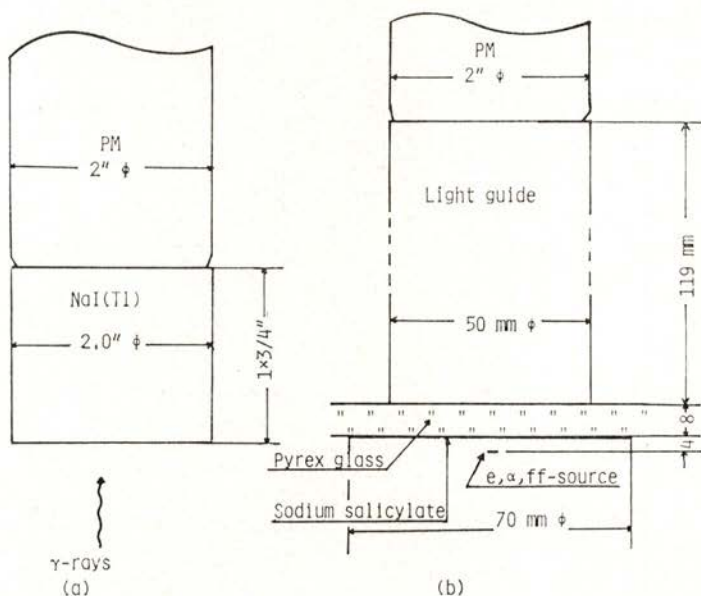


Fig. 14 — Geometrical arrangements of the apparatus for liquid argon and xenon (a), and for NaI(Tl) crystal detector (b) used in the measurements for Table 5.

In particular, the reduction of scintillation yield due to fission fragments in NaI (Tl) crystals is remarkable compared with that in liquid argon. This means that the quenching effect in the high specific ionization region in liquid argon is smaller than that in NaI (Tl) crystals.

For comparison of the scintillation yield in liquid argon with that in NaI (Tl) crystals, let us try to estimate the rela-



tive light yields from the widths of the pulse height distributions of scintillations from liquid argon, liquid xenon and NaI (Tl) crystals. The apparatus used for observation of scintillation from liquid rare gases is shown in Figure 14 as well as one used for the NaI (Tl) detector. As seen from the figure, we used sodium salicylate film, whose conversion efficiency to visible photons is nearly constant over a wide range of wave lengths, coated on the surface of a Pyrex glass window as wave length shifter. The resolution (fwhm) of scintillation light due to alpha-particles expressed in % for liquid argon and liquid xenon are shown in Table 5 as well as that of 1 MeV gamma-

TABLE 5—Comparison of the energy resolution and the light yield for liquid argon or liquid xenon scintillation counters and NaI (Tl) detectors.

Scintillator	Energy resolution (fwhm) for 6 MeV alpha-particles	Energy resolution (fwhm) for 1 MeV electrons	Relative light yield
Liquid Ar	$10.3 \pm 0.5 \%$	(25.2 %) (*)	$1.08 \begin{matrix} + 1.92 \\ - 0.52 \end{matrix}$ (**)
Liquid Xe	$9.1 \pm 0.5 \%$	(22.3 %) (*)	$1.37 \begin{matrix} + 2.44 \\ - 0.67 \end{matrix}$ (**)
NaI (Tl)		6.0 %	1.00

(\*) These values were estimated from the energy resolutions for 6 MeV alpha-particles.

(\*\*) These errors arise from the uncertainties of light reduction factors in the light guide and conversion efficiencies of sodium salicylate used in the measurement.

-rays in the NaI (Tl) detector. From these values, the relative photon intensity ratio for argon and xenon,  $S_{Xe}/S_{Ar}$  is estimated to be 1.27, assuming that the resolution is proportional to the square root of the number of emitted photons. This value is in fairly good agreement with the theoretical one estimated from  $N_{ex}/N_i$  and  $W_{liq}$  (\*). Also, the last column in the table shows the relative scintillation yields of liquid argon and liquid xenon,

$$(*) \text{ Namely, } \frac{S_{Xe}}{S_{Ar}} = \frac{W_{liqAr} (1 + N_{ex}/N_i)_{Xe}}{W_{liqXe} (1 + N_{ex}/N_i)_{Ar}} = 1.32$$

when the scintillation yield of NaI (T1) crystal is assumed to be unity. In this estimation, also, we assumed that the fraction of photons incident upon the surface of sodium salicylate to the total number of photons is 0.42, the conversion efficiency of sodium salicylate to visible photons is  $0.5 \pm 0.2$  and the reduction factor of light in the light guide is  $0.5 \pm 0.2$ . These results show that the relative scintillation yields per unit absorbed energy for liquid argon and liquid xenon are comparable to that of NaI (T1) crystals.

TABLE 6— $\tau_1$ ,  $\tau_2$  and  $A_1/A_2$  for scintillations from liquid argon, krypton and xenon, excited by fast electrons and alpha particles.

Liquid (Temperature)	Excitation (Ref. n.º)	Electric field (kV/cm)	$\tau_1$ (ns)	$\tau_2$ (ns)	$A_1/A_2$
Liquid Ar (94K)	e(Ref. 64)	6	5.0	860	7.8
»	e( » )	0	6.3	1020	13.5
»	e(Ref. 67)	0	2.4	1100	14.6
(90-100K)	e(Ref. 68)	0	4.6	1540	
» »	$\alpha$ ( » )	0	4.4	1100	
Liquid Kr (120K)	e(Ref. 64)	4	2.1	80	0.9
»	e( » )	0	2.0	91	0.4
»	e(Ref. 67)	0	2.0	85	0.49
Liquid Xe (179K)	e(Ref. 64)	4	2.2	27	0.6
»	e( » )	0		34	
»	$\alpha$ (Ref. 67)	0	3.0	22	25
»	$\alpha$ (Ref. 66)	0	4.0	27	

The counting rate capability of scintillation counters is limited by the decay time of the scintillation. The scintillation from liquid rare gases has two decay components of a few nano-seconds and a few microseconds, which correspond to the life times of the singlet state and the triplet state of the excited molecule, respectively. Table 6 shows both decay time constants  $\tau_1$  and  $\tau_2$  for scintillations from liquid argon, liquid krypton and liquid xenon, excited by fast electrons or alpha-particles, and the ratio between both amplitudes when the decay is expres-



sed by  $A_1 \exp(-t/\tau_1) + A_2 \exp(-t/\tau_2)$  [64-68]. The time constants quoted in the table show small variations for the various measurements. However, the difference in  $\tau_2$  in liquid xenon excited by fast electrons and alpha-particles is caused by recombination between electrons and ions. In the case of electron excitation, the time required for recombination  $\tau_r$  is longer than  $\tau_1$  and comparable to  $\tau_2$  in liquid xenon. So, if a high electric field is applied, the component due to recombination does not appear. For the alpha-particle excitation, such a slow component does not appear because the recombination rapidly occurs due to the high density of electron-ion pairs produced by this particle. On the other hand, in liquid argon, this phenomenon is not seen because  $\tau_r$  is shorter than  $\tau_1$  even for the electron excitation.

Recently, Kubota et al. [67] observed a decrease in the decay times for the slow component with an addition of Xe (>1ppm), N<sub>2</sub> (~2 %) or CO<sub>2</sub> (~1 %) in liquid argon excited by fast electrons. Such a mixing effect is promising for application to scintillation counters with fast time response.

The scintillation yields in liquid argon and liquid xenon are comparable to those in NaI (Tl) crystals and the dE/dx-dependence of the scintillation yield is smaller. Also, these liquid scintillators have a faster time response than NaI (Tl) detectors. However, a considerable percentage of the photons emitted in the scintillators is absorbed by surrounding materials, because there are no good reflectors for ultraviolet photons. At present, therefore, we can not achieve a good energy resolution by liquid rare gas scintillators. If a wave length shifter that can be doped into liquid rare gases without any quenching effect is found the above difficulty may be overcome.

## 5.2 — *Proportional scintillation*

In the gas scintillation proportional counter «photon-multiplication» occurs along the path of a drifting electron in the region of high electric field around the center wire. This is called «proportional scintillation», because the intensity is proportional to the number of electrons initially produced by ionizing radiation. In liquid rare gases, we found that such a proportional scintilla-

tion occurs only in liquid xenon. The photons in the proportional scintillation are emitted from deexcitation of excited molecules to the dissociative ground state, as in the direct scintillation. The proportional scintillation is produced only in the region very close to the surface of the center wire. Therefore, the rise time of the scintillation is comparable to or slightly longer than that of the direct scintillation, if the range of an incident particle is negligibly small. Accordingly, a counting rate of  $10^5$  counts/sec will be achievable in proportional scintillation as in direct scintillation. These properties show that the proportional scintillation counter is suitable as a position sensitive detector with fast time response as well as a proportional counter. If the gain of photon-multiplication is sufficient, furthermore, it is expected that in principle a good energy resolution for gamma-rays, as determined only by the Fano factor, is achievable as in gas proportional scintillation counters for X-ray detection [69]. This means that by the use of the proportional scintillation, a liquid xenon gamma-ray spectrometer with a high energy resolution, which is not affected by the electronic noise of the preamplifier, can be developed.

From the same point of view, we measured the light gain versus the voltage applied to the center wire for liquid xenon proportional scintillation counters with different center wires of 4, 6, 8.5, 10, 11 and 20  $\mu\text{m}$  in diameter [28]. The results are shown in Figure 15 as well as the curves of charge gain. From the analysis of these results, we found that the increase in the photon gain with the applied voltage in liquid xenon is approximately explained by assuming the linear relation between the photon gain and the electric field strength as in gaseous xenon; and the threshold field strength for production of photons in liquid xenon ( $4 - 7 \times 10^5$  V/cm) is nearly equal to the value calculated by considering liquid xenon as gaseous xenon of 520 atm. Also, the number of photons emitted by one electron in the proportional scintillation process was estimated to be about five for a 20  $\mu\text{m}$  wire at the applied voltage of 5 kV. This means that if a center wire of 50  $\mu\text{m}$  in diameter is used in a proportional counter and 12 kV is applied the photon gain per one electron is expected to be about 30 [70]. This value is large enough to make the electronic noise effect negligible.



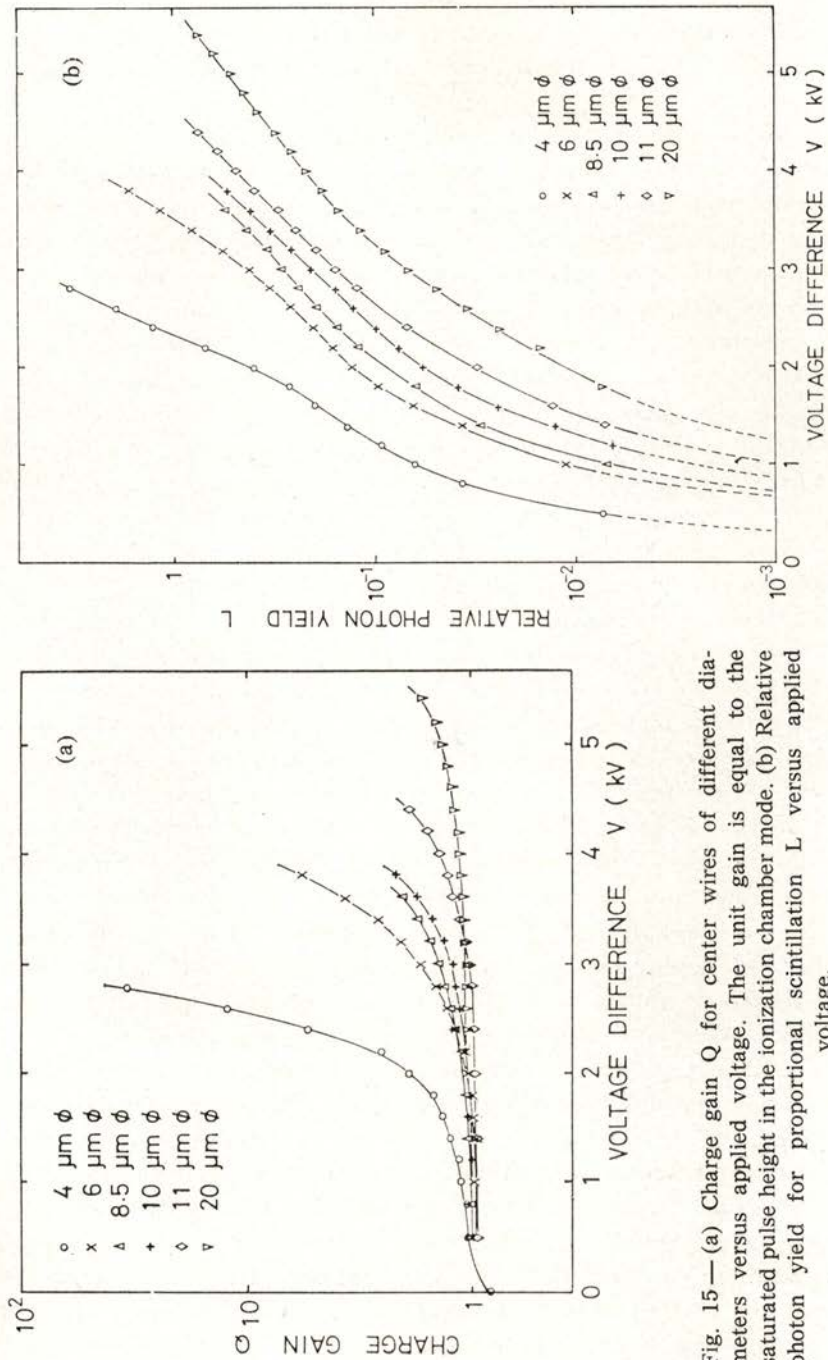


Fig. 15—(a) Charge gain  $Q$  for center wires of different diameters versus applied voltage. The unit gain is equal to the saturated pulse yield in the ionization chamber mode. (b) Relative photon yield for proportional scintillation  $L$  versus applied voltage.

## 6 — POSSIBILITIES OF APPLICATION TO NUCLEAR RADIATION DETECTORS

Some possibilities of application of liquid rare gases to nuclear radiation detectors have already been described in each section. Here, they are summarized as a whole and some ideas for developing liquid rare gases detectors are presented. Liquid rare gases can be used as detector media in the following four detector modes as in gaseous detectors; i) ionization mode, ii) scintillation mode, iii) proportional scintillation mode and iv) proportional ionization mode. In the modes, i) and iii) they will be used as energy spectrometers with good energy resolution or as position sensitive detectors with good position resolution for minimum ionizing particles or gamma-rays. Mode ii) will correspond to fast counters or detectors for heavy ions. In the mode iv) they will be used only as position sensitive detectors, because its signals are useful only for timing.

Now, let us consider in detail the possibilities of application to nuclear radiation detectors of liquid argon and liquid xenon.

In liquid argon, the photon- and electron-multiplications do not occur as mentioned before, and so, liquid argon can be used only as detector medium in the ionization and scintillation modes. Nevertheless, it is expected to be a good detector medium in large size detectors, such as calorimeters for energy measurement of high energy gamma-rays or high energy electrons and time projection chambers for neutrino detection, because of its cheapness and the easiness of its treatment. Recently, the possibility of «photo-ionization detectors» in liquid phase was suggested by Policarpo [70]. The most practical medium for this type of detector is liquid argon doped by a small amount (~ several ten ppm) of organic compounds with low ionization potential. Such a liquid photo-ionization detector (LPID) is expected to have a large detection efficiency over a wide wavelength range of ultra-violet photons and a better position resolution than gaseous PID.

On the other hand, it is not so easy to construct a large size liquid xenon detector as compared with liquid argon, because of its high cost and its high sensitivity to impurities. However, liquid xenon is suitable as detector medium for gamma-ray detectors, because of its high atomic number and



its high atomic density. As a gamma-ray spectrometer with good energy resolution, a gridded ionization chamber or a proportional scintillation chamber filled with liquid xenon may be used. Also, liquid xenon is suitable as detector medium in the drift chamber, because the drift velocity of electrons in liquid xenon is almost constant for electric fields higher than 3 kV/cm. If a liquid xenon proportional scintillation chamber is used with a liquid xenon PID, we can use the detector system as a position sensitive detector as well as an energy spectrometer for gamma-rays. Furthermore, it is possible to construct a kind of time projection chamber for gamma-rays by combining drift chambers and gridded ionization techniques.

Finally, we would like to suggest a new type liquid rare gas detector, which uses both signals of ionization and scintillation. Considerable part of the scintillation from liquid rare gases arises from recombination between electrons and ions. In particular, this is remarkable for heavy ions. On the other hand, only a small amount of charge produced by a heavy ion is observable. Thus, the scintillation signal and charge signal are complementary for heavy charged particles and it is considered that some linear combination of scintillation signal and charge signal will be proportional to the energy of the particle. Such a detector will be useful as a total absorption detector for high energy heavy ions. Also, the ratio of the scintillation signal to the charge signal depends on the kind of particle. Therefore, such a technique may be used for particle identification of heavy ions.

#### ACKNOWLEDGMENT

The author would like to express his thanks to Professor A. J. P. L. Policarpo for having made possible the realization of this review article.

#### REFERENCES

- [1] L. W. ALVAREZ, *Lawrence Radiation Laboratory Physics Note*, No. 672 (1968).
- [2] R. A. MULLER, S. E. DERENZO, G. SMADJA, B. SMITH, R. G. SMITS, H. ZAKLAD and L. W. ALVAREZ, *Phys. Rev. Letters*, **27**, 532 (1971).
- [3] S. E. DERENZO, T. S. MAST, H. ZAKLAD and R. A. MULLER, *Phys. Rev.*, **A9**, 2582 (1974).

- [4] S. E. DERENZO, A. R. KIRSCHBAUM, P. H. EBERHARD, R. R. ROSS and F. T. SOLMITZ, *Nucl. Instr. Meth.*, **122**, 319 (1974).
- [5] M. C. GADENNE, A. LANSIART and A. SEIGNEUR, *Nucl. Instr. Meth.*, **124**, 521 (1975).
- [6] J. PRUNIER, R. ALLEMAND, M. LAVAL and G. THOMAS, *Nucl. Instr. Meth.*, **109**, 257 (1973).
- [7] A. LANSIART, A. SEIGNEUR, J. MORETTI and J. MORUCCI, *Nucl. Instr. Meth.*, **135**, 47 (1976).
- [8] B. A. DOLGOSHEIN, V. N. LEBEDENKO and B. U. RODIONOV, *JETP Letters*, **11**, 351 (1970).
- [9] B. A. DOLGOSHEIN, A. A. KRUGLOV, V. N. LEBEDENKO, V. P. MIROSHICHENKO and B. U. RODIONOV, *Sov. J. Particles Nucl.*, **4**, 70 (1973).
- [10] G. KNIES and D. NEUFFER, *Nucl. Instr. Meth.*, **120**, 1 (1974).
- [11] J. ENGLER, B. FRIEND, W. HOFMANN, H. KLEIN, R. NICKSON, W. SCHMIDT-PARZEFALL, A. SEGAR, M. TYRRELL, D. WEGENER, T. WILLARD and K. WINTER, *Nucl. Instr. Meth.*, **120**, 157 (1974).
- [12] W. J. WILLIS and V. RADEKA, *Nucl. Instr. Meth.*, **120**, 221 (1974).
- [13] D. HITLIN, J. F. MARTIN, C. C. MOREHOUSE, G. S. ABRAMS, D. BRIGGS, W. CARITHERS, S. COOPER, R. DEVOE, C. FRIEDBERG, D. MARSH, S. SHANNON, E. VELLA and J. S. WHITAKER, *Nucl. Instr. Meth.*, **137**, 225 (1976).
- [14] C. J. FABJAN, W. STRUCZINSKI, W. J. WILLIS, C. KOURKOUHELIES, A. J. LANKFORD and P. REHAK, *Nucl. Instr. Meth.*, **141**, 61 (1977).
- [15] C. CERRI and F. SERGIAMPRIETRI, *Nucl. Instr. Meth.*, **141**, 207 (1977).
- [16] C. RUBBIA, *CERN EP Internal Report*, 77-8 (1977).
- [17] H. H. CHEN and J. F. LATHROP, *Nucl. Instr. Meth.*, **150**, 585 (1978).
- [18] H. H. CHEN and P. J. DOE, *IEEE Transaction on Nucl. Sci.*, **NS-28** 454 (1980).
- [19] S. KONNO and S. KOBAYASHI, *Sci. Pap. Inst. Phys. Chem. Res.*, **67**, 57 (1973).
- [20] T. TAKAHASHI, S. KONNO and T. DOKE, *J. Phys.* **C7**, 230 (1974).
- [21] M. MIYAJIMA, T. TAKAHASHI, S. KONNO, T. HAMADA, S. KUBOTA, E. SHIBAMURA and T. DOKE, *Phys. Rev.*, **A9**, 1438 (1974).
- [22] T. TAKAHASHI, S. KONNO, T. HAMADA, S. KUBOTA, A. NAKAMOTO, A. HITACHI, E. SHIBAMURA and T. DOKE, *Phys. Rev.*, **A12**, 1771 (1975).
- [23] E. SHIBAMURA, A. HITACHI, T. DOKE, T. TAKAHASHI, S. KUBOTA and M. MIYAJIMA, *Nucl. Instr. Meth.*, **131**, 249 (1975).
- [24] S. KUBOTA, A. NAKAMOTO, T. TAKAHASHI, S. KONNO, T. HAMADA, M. MIYAJIMA, E. SHIBAMURA, A. HITACHI and T. DOKE, *Phys. Rev.*, **B13**, 1649 (1976).
- [25] T. DOKE, A. HITACHI, S. KUBOTA, A. NAKAMOTO and T. TAKAHASHI, *Nucl. Instr. Meth.*, **134**, 353 (1976).
- [26] E. SHIBAMURA, S. KUBOTA, T. TAKAHASHI and T. DOKE, *Phys. Rev.*, **A20**, 2547 (1979).
- [27] M. MIYAJIMA, K. MASUDA, Y. HOSHI, T. DOKE, T. TAKAHASHI, T. HAMADĀ, S. KUBOTA, A. NAKAMOTO and E. SHIBAMURA, *Nucl. Instr. Meth.*, **160**, 239 (1979).



- [28] K. MASUDA, S. TAKASU, T. DOKE, T. TAKAHASHI, A. NAKAMOTO, S. KUBOTA and E. SHIBAMURA, *Nucl. Instr. Meth.*, **160**, 247 (1979).
- [29] K. MASUDA, A. HITACHI, Y. HOSHI, T. DOKE, A. NAKAMOTO, E. SHIBAMURA and T. TAKAHASHI, *Nucl. Instr. Meth.*, **174**, 439 (1980).
- [30] K. MASUDA, T. TAKAHASHI and T. DOKE, *Nucl. Instr. Meth.* (to be published).
- [31] H. A. ULLMAIER, *Phys. Med. Biol.*, **11**, 95 (1966).
- [32] N. V. KLASSEN and W. F. SCHMIDT, *Can. J. Chem.*, **47**, 4286 (1969).
- [33] M. G. ROBINSON and G. R. FREEMAN., *Can. J. Chem.*, **51**, 641 (1973).
- [34] S. HUANG and G. R. FREEMAN, *Can. J. Chem.*, **55**, 1838 (1977).
- [35] R. L. PLATZMAN, *Int. J. Appl. Rad. Isotopes*, **10**, 116 (1961).
- [36] W. SHOCKLEY, *Czech. J. Phys.*, **B11**, 81 (1961).
- [37] C. A. KLEIN, *J. Appl. Phys.*, **39**, 2029 (1968).
- [38] G. BALDINI and R. S. KNOX, *Phys. Rev. Letters*, **11**, 127 (1963).  
G. BALDINI, *Phys. Rev.*, **137**, A508 (1965).
- [39] U. ROSSLER, *Phys. Status Solidi* **B42**, 345 (1970), **B45**, 483 (1971).
- [40] G. KEITEL, DESY F41-70/7 (1970).  
P. SCHREBER, DESY F1-70/5 (1970).
- [41] U. FANO, *Phys. Rev.*, **72**, 26 (1947).
- [42] G. D. ALKHAZOV, A. P. KOMAR and A. A. VOROBEV, *Nucl. Instr. Meth.*, **48**, 1 (1967).
- [43] H. A. BETHE and J. ASHKIN, *Experimental Nuclear Physics* (ed. E. Segre, Wiley, New York, 1973) Vol. 1, Part 2.
- [44] I. M. OBODOVSKY and S. G. POKACHALOV, *Low Temp. Phys.*, **5**, 829 (1979).
- [45] A. P. PISAREV, *Sov. Phys. JETP*, **36**, 823 (1973).
- [46] E. SHIBAMURA, A. HITACHI, M. MIYAJIMA, S. KUBOTA, A. NAKAMOTO, T. TAKAHASHI, S. KONNO and T. DOKE, *Bull. Sci. Eng. Res. Lab. Waseda Univ.*, **69**, 104 (1975).
- [47] S. E. DERENZO, D. B. SMITH, R. G. SMITS, H. ZAKLAD, L. W. ALVAREZ and R. A. MULLER, UCRL-20118 (1970).
- [48] M. MIYAJIMA, K. MASUDA, A. HITACHI, T. DOKE, T. TAKAHASHI, S. KONNO, T. HAMADA, S. KUBOTA, A. NAKAMOTO and E. SHIBAMURA, *Nucl. Instr. Meth.*, **134**, 403 (1976).
- [49] L. ONSAGER, *Phys. Rev.*, **54**, 554 (1938).
- [50] T. TAKAHASHI, S. KONNO, A. HITACHI, T. HAMADA, A. NAKAMOTO, M. MIYAJIMA, E. SHIBAMURA, Y. HOSHI, K. MASUDA and T. DOKE, *Sci. Pap. Inst. Phys. Chem. Res.*, **74**, 65 (1980).
- [51] H. ZAKLAD, UCRL-20690 (1971).
- [52] W. HOFMANN, U. KLEIN, M. SCHULZ, J. SPENGLER and D. WEGENER, *Nucl. Instr. Meth.*, **135**, 151 (1976).
- [53] G. BAKALE, U. SOWADA and W. F. SCHMIDT, *J. Phys. Chem.*, **80**, 2556 (1976).
- [54] J. L. PACK, R. E. VOSHALL and A. V. PHELPS, *Phys. Rev.*, **127**, 2084 (1962).
- [55] L. S. MILLER, S. HOWE and W. E. SPEAR, *Phys. Rev.*, **166**, 871 (1968).
- [56] Y. YOSHINO, U. SOWADA and W. F. SCHMIDT, *Phys. Rev.*, **A14**, 438 (1976).

- [57] E. SHIBAMURA, S. KUBOTA, T. TAKAHASHI and T. DOKE, *Proc. Int. Seminar on Swarm Experiments in Atomic Collision Research*, Tokyo, 47 (1979).
- [58] J. LEKNER, *Phys. Rev.*, **158**, 130 (1967).
- [59] J. A. NORTHROP and J. C. GURSKY, *Nucl. Instr. Meth.*, **3**, 207 (1958).
- [60] S. KUBOTA, A. NAKAMOTO, T. TAKAHASHI, T. HAMADA, E. SHIBAMURA, M. MIYAJIMA, K. MASUDA and T. DOKE, *Phys. Rev.* **B17**, 2762 (1978).
- [61] A. HITACHI, T. TAKAHASHI, T. HAMADA, E. SHIBAMURA, A. NAKAMOTO, N. FUNAYAMA, K. MASUDA and T. DOKE, *Phys. Rev.*, **B23**, (1981) in press.
- [62] A. HITACHI, T. TAKAHASHI, T. HAMADA, E. SHIBAMURA, N. FUNAYAMA, K. MASUDA, J. KIKUCHI and T. DOKE, *Proc. INS Intern. Symposium on Nuclear Radiation Detectors*, Tokyo, (1981) in press.
- [63] R. B. MURRAY and A. MEYER, *Phys. Rev.*, **122**, 815 (1961).
- [64] S. KUBOTA, M. HISHIDA and J. RUAN, *J. Phys.*, **C11**, 2645 (1978).
- [65] S. KUBOTA, M. HISHIDA, M. SUZUKI and J. RUAN, *Phys. Rev.*, **B20**, 3486 (1979).
- [66] S. KUBOTA, M. SUZUKI and J. RUAN, *Phys. Rev.* **B21**, 2632 (1980).
- [67] S. KUBOTA, M. HISHIDA, M. SUZUKI and J. RUAN, *Proc. INS Intern. Symposium on Nuclear Radiation Detectors*, Tokyo, (1981) in press.
- [68] M. J. CARVALHO and G. KLEIN, *J. Luminescence*, **18/19**, 487 (1979).
- [69] A. J. P. L. POLICARPO, M. A. F. ALVES, M. C. M. DOS SANTOS and M. J. T. CARVALHO, *Nucl. Instr. Meth.*, **102**, 337 (1972).
- [70] A. J. P. L. POLICARPO, *Proc. INS Intern. Symposium on Nuclear Radiation Detectors*, Tokyo, (1981) in press.